THE JOURNAL OF PHYSICAL CHEMISTRY C

Article

Cite This: J. Phys. Chem. C XXXX, XXX, XXX–XXX

pubs.acs.org/JPCC

Temperature-Programmed Desorption for Isotope Separation in Nanoporous Materials

Stephen A. Fitzgerald,*[†] Kai Shinbrough,[†] Katharine H. Rigdon,[†] Jesse L. C. Rowsell,[‡] Matthew T. Kapelewski,[¶] Simon H. Pang,[§] Keith V. Lawler,[∥] and Paul M. Forster[∥]

[†]Department of Physics and Astronomy, Oberlin College, Oberlin, Ohio 44074, United States

[‡]Department of Chemistry and Biochemistry, Oberlin College, Oberlin, Ohio 44074, United States

[¶]Department of Chemistry, University of California, Berkeley, Berkeley, California 94720, United States

[§]School of Chemical & Biomolecular Engineering, Georgia Institute of Technology, Atlanta, Georgia 30332, United States

[∥]High Pressure Science and Engineering Center, University of Nevada Las Vegas, Las Vegas, Nevada 89154, United States

Supporting Information

ABSTRACT: Hydrogen isotope separation based on differences in quantum zero-point energy was investigated using a novel temperature-programmed desorption approach. Spectra obtained as a function of hydrogen concentration reveal multiple distinct binding sites that correlate with the crystallographic structure of the particular material. In each case, the higher mass isotope desorbs at a characteristic temperature higher than that of the lower mass counterpart. Materials with greater binding energy exhibit a larger difference in characteristic temperature between D_2 and H_2 but also a broader desorption profile. Simulations based on the standard Polanyi–Wigner equation reveal this broadening to be an intrinsic property present in all higher binding energy materials. As such, the key factor in temperature desorption separation is not the absolute difference in binding energy of the two species but rather the fractional difference.

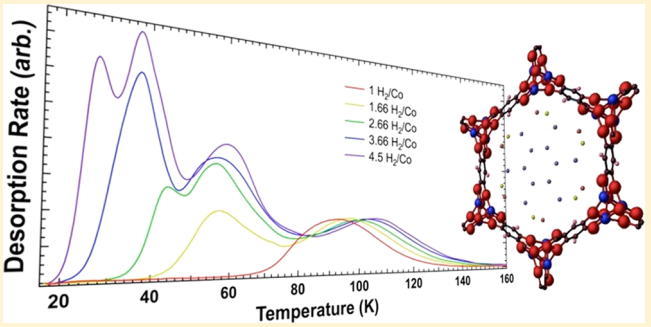

INTRODUCTION

Soon after its discovery in 1931,[1] it was realized that deuterium would have applications within biomedical research.[2] The medical usage has grown with time,[3,4] and deuterium is now used extensively in other industries, including nuclear power generation[5] and chemical labeling.[6,7] However, because deuterium makes up less than 0.02% of naturally occurring hydrogen, its extraction has always been a limiting factor for its usage.

The separation of isotopes is, given their chemical similarity, quite challenging, and existing industrial methods are either highly energy inefficient or operate with a low selectivity.[5] Thus, new methods are being proposed, and most recently, a separation approach based on the difference in the quantum behavior of H_2 and D_2 confined within nanoporous materials has emerged.[8−11] In particular, metal−organic frameworks (MOFs) have been shown to separate deuterium from hydrogen[9,11−13] with reported selectivities as high as 12 at 60 K.[9] This is promising given that the main industrial separation method operates with a selectivity of ∼2 at room temperature.[5] With the vast number of possible MOF structures, there is hope that optimized materials can be synthesized with even higher selectivities that operate close to room temperature, thus providing a new separation technology.

Proposed quantum-based separations in nanoporous materials exploit both kinetic and thermodynamic effects. Kinetic separations utilize the mass dependence of diffusion rates, while the thermodynamic approach relies on the fact that D_2, being more massive, has a smaller zero-point energy and is preferentially adsorbed over H_2.[8−11] In the traditional thermodynamic approach, a low pressure gas stream is allowed to flow over the porous adsorbent until saturation, at which point the adsorbed molecules are collected either through heating or evacuation. In this paper, we examine a modified degassing step that could be used to further enhance this separation process.

Temperature-programmed desorption (TPD) is most commonly used as an analysis tool.[14] After adsorption, the adsorbent's temperature is increased at a constant rate, and the degassing of adsorbates is monitored using a mass spectrometer. The desorption rate plotted as a function of temperature provides information about adsorbate−adsorbent interactions; in particular, TPD spectra provide information on a site's binding energy, abundance, and behavior with different isotopes. However, TPD could also be used as an additional

Received: November 9, 2017
Revised: January 3, 2018
Published: January 4, 2018

DOI: 10.1021/acs.jpcc.7b11048
J. Phys. Chem. C XXXX, XXX, XXX–XXX

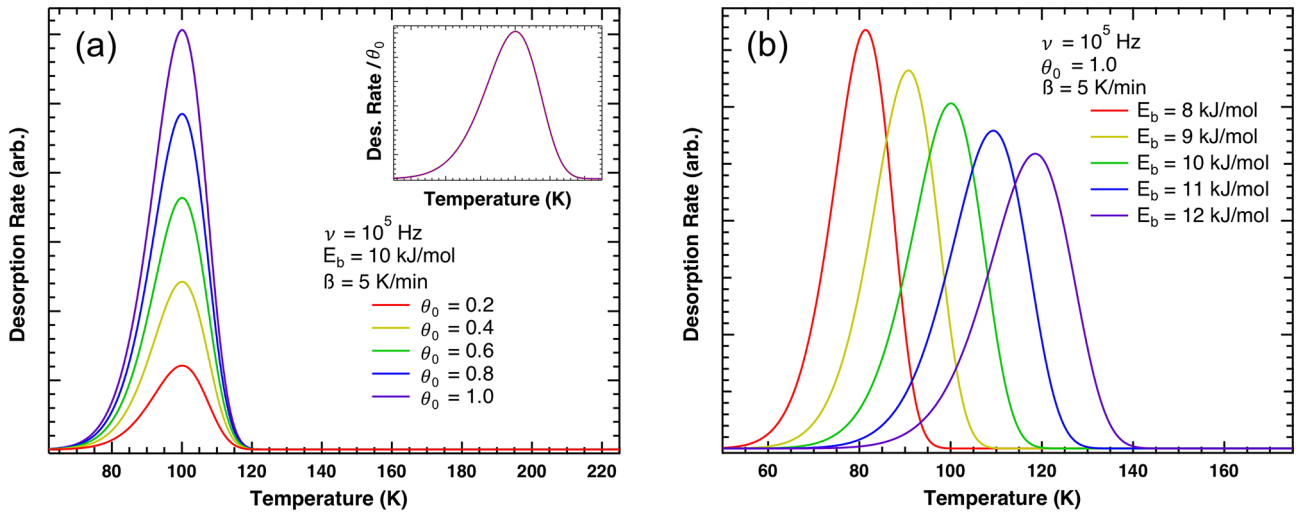

Figure 1. Runge–Kutta numerical solutions to the first-order, coverage-independent Polanyi–Wigner equation for systematically varying (a) initial surface coverage θ_0 and (b) binding energy E_b.

separation method. During heating, less massive isotopes desorb at a lower temperature due to their weaker adsorption enthalpy. At an optimal temperature, the resulting gaseous mixture which is depleted of higher mass isotopes can be evacuated, leaving behind an adsorbed phase mixture enriched in higher mass isotopes.

In the next section, we briefly present a background on TPD along with a series of simulations that guide the proposed separation process. The experimental procedure shows how a pressure gauge can be used to obtain desorption profiles that would normally require a specialized mass spectrometer. Results are first presented for nanoporous material Co_2(dobdc), showing the ability of our approach to reveal different binding energy sites within a material. Experimental desorption profiles agree with simulation with respect to binding energy dependence. The practicality of the temperature-programmed separation method is then analyzed. We find that stronger binding energy materials shift the desorption profile closer to room temperature (an industrial benefit) and produce a greater difference in the characteristic desorption temperature between D_2 and H_2. However, their ability to separate via TPD is limited by the inherent temperature broadening of the desorption profiles. A much more effective separation occurs for materials with a large difference in binding energy between D_2 and H_2 but with a relatively modest binding energy. Experimental data for materials Co_2(dobdc), Co_2(*m*-dobdc), ZIF-8, and VSB-5 are shown to be consistent with the model predictions.

Temperature-Desorption Simulations. Temperature-programmed desorption is a technique originally developed to understand surface desorption kinetics.[15] However, in the past two decades, a body of research has emerged applying TPD to the desorption of molecules adsorbed into three-dimensional, nanoporous adsorbents.[9,11,16−19]

The procedure for TPD experiments is simple: adsorb a species into (or onto) an adsorbent, heat the material at a constant rate, and record the desorption rate of the species as a function of temperature. For surfaces, this desorption rate follows an Arrhenius expression called the Polanyi–Wigner equation:[14]

$$r(T) = -\frac{d\theta}{dt} = \nu\theta^n e^{-E_b/k_B T} \quad (1)$$

where r is the desorption rate of the species from the adsorbent, T the temperature of the material, θ the fractional surface coverage of the species, t time, ν the pre-exponential factor with units of frequency, n the order of desorption, E_b the binding energy of the species to the adsorbent, and k_B Boltzmann's constant. T and t are related by the constant heating rate $\beta = dT/dt$. In its general form, the Polanyi–Wigner equation expresses ν and E_b as functions of coverage (θ) and other variables. Here, we concern ourselves with the coverage-independent form.

In Figure 1a, we present numerical solutions to the first-order, coverage-independent Polanyi–Wigner equation evaluated at systematically varying values of θ_0, the initial fractional coverage. We use the Runge–Kutta method in generating these solutions. The solutions are single peaks that simply scale with increasing initial surface coverage such that all the curves lie on top of each other when divided by initial coverage (see inset). In contrast (see Figure 1b), increasing binding energy E_b causes the peak to broaden and shift to higher temperature. These simulations are consistent with earlier work[14] and illustrate both the advantages and limitations of using strongly binding materials for TPD separations.

Experimental Procedure. In this work, we present data acquired with a novel form of TPD. Traditionally, TPD is performed with a mass spectrometer (or less commonly through gas chromatography in conjunction with a thermal conductivity detector) that detects species as they desorb and evacuates them from the system. Here, we show that physically informative TPD spectra can be acquired with a nonevacuative approach, simply using a pressure gauge. As suitable mass spectrometers cost in excess of 75,000 USD (private communication), require calibration, and must deal with an H_2O background alias at 2 amu, the acquisition of TPD spectra using a far simpler and less costly method is an important development.

The synthesis and characterization of the Co_2(dobdc), Co_2(*m*-dobdc), ZIF-8, and VSB-5 samples used in this paper were presented in our previous work.[10,20−22] A custom-built cryogenic chamber allows sample powders to be mounted,

DOI: 10.1021/acs.jpcc.7b11048
J. Phys. Chem. C XXXX, XXX, XXX−XXX

degassed, cooled, and dosed with hydrogen without exposing them to air.[23] The apparatus is comprised chiefly of a modified liquid helium Janis ST-300T closed cycle cryostat and a Micromeritics ASAP 2020 physisorption analyzer. The sample temperature is maintained using a Lakeshore Model 331 controller with two DT-670 silicon diode temperature sensors. A small quantity of helium gas is used to ensure thermal contact between the sample powder, copper cell, and thermometer. The ASAP device doses a known amount of hydrogen gas and monitors the pressure of the system during desorption using two capacitance manometers (with ranges of 10^{-6} to 10^{-2} bar and 10^{-3} to 1 bar). Research grade >99.99% pure H_2, D_2, and He are used.

Because the sample mass (typically ∼10 mg), crystalline structure, and gas dosing amount are all known, this custom apparatus permits analysis of desorption behavior as a function of initial adsorbed species concentration. This allows us to extract site-specific adsorption information that can be analyzed in conjunction with neutron diffraction data,[24] which provides the crystallographic location of the adsorption sites.

Gas dosings are typically performed at ∼77 K. Hydrogen is loaded from a 40 cm^3 volume at pressures in the range of 5−100 mbar. The sample is then cooled at a rate of 5 K/min to a temperature of ∼15 K, at which point nearly all the hydrogen is adsorbed. The sample is allowed to equilibrate for 1 h before acquisition of a temperature-desorption spectrum with a heat rate of 5 K/min. A schematic of the experimental setup is shown in Figure S1 of the Supporting Information.

RESULTS AND DISCUSSION

Establishing Adsorption Sites. As we show below, a simple pressure-based TPD approach can establish the presence of multiple adsorption sites of differing adsorption properties within a given material. Spectra are presented in terms of the desorption rate, obtained by numerical differentiation of the gas concentration (as measured by the pressure gauge in conjunction with the ideal gas law). Figure 2 shows these temperature-desorption spectra for a series of adsorbed hydrogen concentrations within the nanoporous material Co_2(dobdc) (dobdc^{4-} = 2,5-dioxido-1,4-benzenedicarboxylate) also known as Co-MOF-74 and CPO-27(Co).[25,26] Neutron diffraction data reported by Liu et al. indicate that the chosen concentrations should successively populate the primary (open-metal), secondary (oxygen), tertiary (benzene), and finally quaternary (liquid-like) adsorption sites within the material, in order of decreasing binding energy strength.[24] The presented temperature-desorption spectra are consistent with this prediction, showing the successive appearance of four desorption peaks. With increasing concentration, each successive peak occurs at a lower temperature, indicating a decrease in site binding strength. In agreement with the simulations in Figure 1b, those peaks arising from hydrogen desorption at higher binding energy sites occur at higher temperature and have broader desorption profiles. This successive site filling model is also confirmed by infrared spectra obtained at low temperature and during the warming process (see Figures S3 and S4).

The spectra reported here are consistent with those acquired using a traditional TPD approach with a mass spectrometer.[9] In ref 9, Oh et al. examined a single desorption spectrum at unknown concentration and observed three distinct peaks with evidence that the lowest-temperature feature could be composed of two peaks. The simple approach presented here

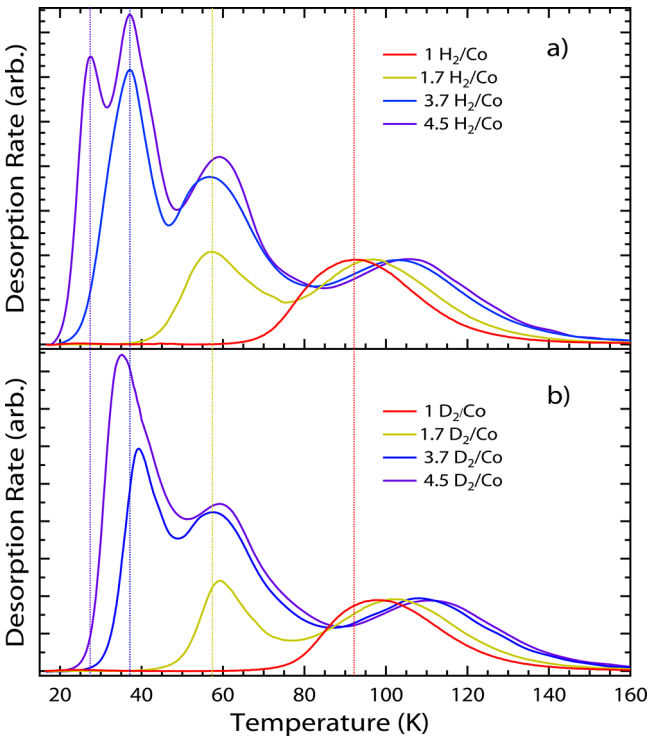

Figure 2. Temperature-desorption spectra of (a) H_2 and (b) D_2 in Co_2(dobdc) for varying initial hydrogen concentration (expressed in terms of adsorbed molecules per cobalt). Four adsorption sites are apparent in the H_2 spectra, in agreement with crystallographic structure of Co_2(dobdc).[24] Dashed lines indicate the H_2 desorption maximum for each peak; the equivalent D_2 peaks occur at slightly higher temperature.

appears to produce slightly better resolved spectra with the added advantage of knowing the concentration of the adsorbed species.

The shift in the primary site desorption profile, and to a lesser extent the other peaks, to higher temperature with increased hydrogen concentration is believed to be an artifact of our approach. Because the desorbed species are not evacuated, the final pressure in the system increases with increasing concentration (in Figure 2, from 20 to 100 mbar). This increase in the final pressure leads to a greater probability of readsorption during the TPD procedure and shifts the peak desorption rate to higher temperature. Readsorption is considered in more detail at the end of the paper when we examine experimental data obtained with different desorption volumes.

The D_2 spectra in Figure 2b show a pattern similar to that of H_2, with the important distinction that the peaks are shifted to higher temperature in comparison to the corresponding H_2 peak. This is illustrated more clearly in Figure S5 where we show just the low concentration data. It is this separation between H_2 and D_2 desorption profiles that determines the efficacy of the proposed separation process. Finally, we note that even at high concentration the D_2 spectra do not exhibit a distinct fourth peak. We believe this is due to the third and fourth peaks in the D_2 spectra being too close in temperature to resolve.

Previous work has established the primary adsorption site in Co_2(dobdc) as corresponding to the so-called "open metal" or coordinatively unsaturated Co site.[24,27] The measured H_2 isosteric heat of adsorption for this site is 10.8 kJ/mol, with

DOI: 10.1021/acs.jpcc.7b11048
J. Phys. Chem. C XXXX, XXX, XXX−XXX

D_2 1.2 kJ/mol higher.[9,20] These open-metal sites produce significantly stronger binding energies for H_2 than do more traditional van der Waals-based sites. This has motivated their study in the effort to increase hydrogen−MOF interactions for practical H_2 storage, reaction catalysis, and optimized gas separation.[9,20,24,27] In particular, as stronger binding sites lead to a greater zero-point energy, it is predicted that they will also lead to a greater ZPE difference between H_2 and D_2, which is in turn predicted to produce more efficient isotope separation.[28]

Efficiency of Temperature-Programmed Separation. As the Polanyi−Wigner equation correctly captures the binding energy dependence of the experimental spectra presented in this work, we investigate the practicality of hydrogen isotope separation in nanoporous materials through simulation based on this equation. For temperature-programmed separation, the ideal desorption profiles of H_2 and D_2 are completely separated (such that the area of overlap of H_2 and D_2 profiles is zero). In this case, a valve could be closed at a temperature after total H_2 desorption, and all of the initially adsorbed D_2 could be retrieved at 100% purity from the adsorbed phase. For profiles that do overlap, temperature-programmed separation necessitates the disposal of a certain fraction of the initially adsorbed D_2 to achieve a desired D_2 purity. Figure 3 presents four sets of

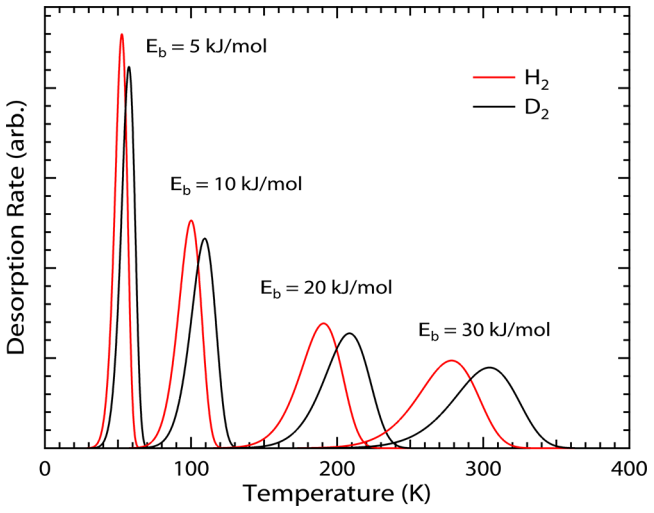

Figure 3. Simulated pairs of H_2 and D_2 temperature-desorption spectra for varying binding energies based on the first-order, coverage-independent Polanyi−Wigner equation and a 10% difference in binding energy between D_2 and H_2.

simulated H_2 and D_2 spectra for a series of binding energies. For each pair of spectra, the binding energy of D_2 is modeled after the experimental trend that shows a roughly 10% increase relative to that of H_2.[10,28] The choice of 10% is also motivated by the linear regression (see Figure S6) arising from the experimental T_{max} values for D_2 and H_2 listed in Table 1.

These profiles show that in principle an arbitrarily large selectivity could still be achieved with this method but at the cost that a significant amount of the initial D_2 is rejected. As expected, the temperature difference in maximum desorption rate between H_2 and D_2, ΔT_{max}, increases with increasing binding energy, but the temperature broadening of both desorption profiles causes the overlap of H_2 and D_2 profiles to remain relatively constant. This limits the benefit of working with stronger binding energy materials.

Table 1. Binding Energies, Temperature of Maximum Desorption Rate (T_{max}) for H_2 and D_2, Difference in T_{max} for H_2 and D_2 (ΔT_{max}), and the fwhm of the Desorption Profile of Each Material Surveyed in This Work[a]

material	binding energy (kJ/mol)	H_2 T_{max} (K)	D_2 T_{max} (K)	ΔT_{max}	fwhm (K)
ZIF-8	4.8[b]	55	58	3	12
Co_2(dobdc)	10.8[c]	93	98	5	32
Co_2(*m*-dobdc)	11.5[c]	97	102	5	35
VSB-5	16.5[d]	127	137	10	46

[a]With increases in T_{max} we observe increases in ΔT_{max} as well as an increase in the fwhm of each desorption profile. [b]Ref 30. [c]Ref 20. [d]Ref 31 and Figure S9.

The selectivity of a process can be defined as the ratio of molar fractions in the adsorbed phase (x) and gas phase (y),[29]

$$S = \frac{x_{D_2}/y_{D_2}}{x_{H_2}/y_{H_2}} = \frac{n_{a,D_2}/n_{a,H_2}}{n_{g,D_2}/n_{g,H_2}} \quad (2)$$

We now define a similar quantity, the enrichment factor, as the ratio of molar fractions in the final recovered mixture to that in the initial mixture.

$$EF = \frac{n_{f,D_2}/n_{f,H_2}}{n_{i,D_2}/n_{i,H_2}} \quad (3)$$

Figure 4 shows the percentage of initial D_2 recovered for enrichment factors of 10, 100, and 1000 as a function of

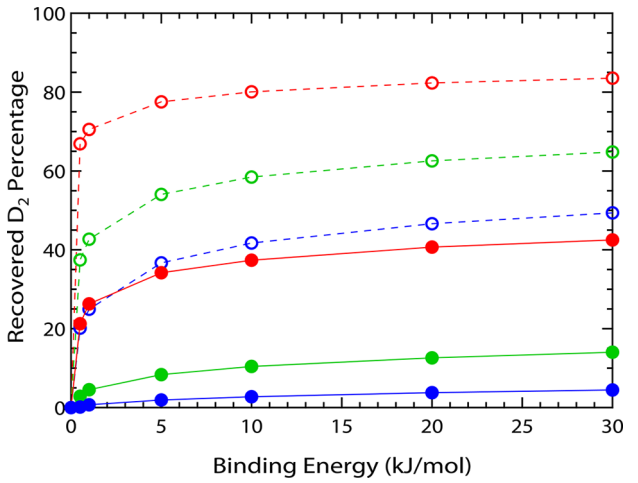

Figure 4. Percentage of initial D_2 recovered for enrichment factors of 10 (red), 100 (green), and 1000 (blue) for simulated temperature-programmed separation. Closed symbols show the case for a 10% difference in binding energy between D_2 and H_2; open symbols show the results for a 20% difference.

binding energy. The results are quite striking and show that a material such as the recently studied Cu(I)MFU-l with a binding energy of ~32 kJ/mol and a D_2 to H_2 difference of 2.7 kJ/mol[28] could in principle achieve an enrichment factor of 1000 but at a cost that less than 4% of the initial D_2 is recovered. Stronger binding energy adsorbents shift the desorption profiles closer to room temperature, which is obviously beneficial from an industrial perspective, and also produce a higher recovery ratio, but as the graph in Figure 4

DOI: 10.1021/acs.jpcc.7b11048
J. Phys. Chem. C XXXX, XXX, XXX−XXX

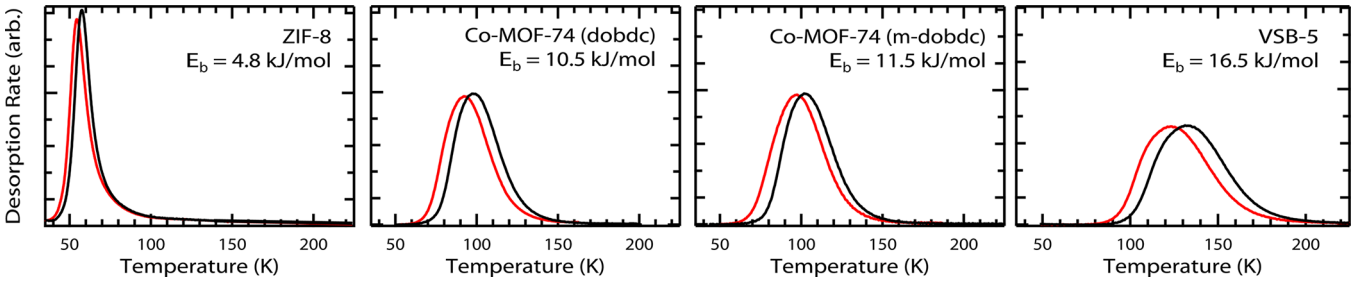

Figure 5. Experimental H_2 (red) and D_2 (black) desorption profiles for nanoporous materials ZIF-8, Co_2(dobdc), Co_2(*m*-dobdc), and VSB-5.

shows, this ratio tends to level off at energies much above 10 kJ/mol.

The limiting factor in separation efficiency arises from the broadening of the desorption profiles for higher binding energies. We thus investigated the behavior of materials with a 20% difference in binding energy between D_2 and H_2 (see open symbols dashed lines in Figure 4). While the trend is similar, the overall efficiency is dramatically better. Even a moderate, 10 kJ/mol, binding energy material with a 20% (2 kJ/mol) difference between D_2 and H_2 performs an order of magnitude better than a 30 kJ/mol material with a 3 kJ/mol difference, recovering 42% of the initial D_2 versus 4.5% with an enrichment factor of 1000.

On the basis of these simulations, the key factor in TPD separation efficiency is not the absolute but rather the fractional difference in binding energy between D_2 and H_2 defined as $\Delta E_b/E_b = (E_{b,D_2} - E_{b,H_2})/E_{b,H_2}$. This would imply that researchers examine materials where the sharpness of the binding potential energy surface is optimized, even at the expense of greater depth.

In this section, we limited our investigation to conditions in which only a single (primary) site is occupied within a material. Similarly, we consider only enrichment during the desorption process and do not address selectivity during the adsorption process. As we showed in our earlier paper, this can be quite large (as high as 5 at 77 K) and would increase the overall enrichment considerably.[10] While our model is highly simplistic (we ignore changes in pre-exponential factor with increasing binding energy and we assume first order desorption), the results are informative and provide a context with which to interpret the experimental data presented in the next section.

Experimental Data for Different Binding Energy Materials. Motivated by the simulations in the previous section, we examined temperature-desorption spectra for a series of nanoporous materials with H_2 binding energies in the range of ~5−16 kJ/mol. For the strongly binding energy materials, we again see evidence for multiple sites that fill sequentially with increasing H_2 concentration (see Figures S7 and S8 of the Supporting Information).

Figure 5 shows the low concentration data for these materials, revealing the primary site behavior for H_2 and D_2 in nanoporous materials ZIF-8,[32] Co_2(dobdc),[25,26] Co_2 (*m*-dobdc),[20] and VSB-5.[22,31,33] The listed binding energies are taken from the literature values for the isosteric heat of adsorption. In a trend similar to simulation, we observe that with increasing binding energy the desorption profiles become broader and shift to a higher characteristic desorption temperature, T_{max} (the temperature at which the desorption rate is a maximum). We observe that the difference in T_{max} between H_2 and D_2, ΔT_{max}, also increases with increasing binding energy. These results are summarized in Table 1. The overall trend is remarkably similar to simulation and confirms that while higher binding energy sites produce a greater separation in characteristic temperature, they also produce broader desorption profiles.

The main difference between simulation and experiment is the presence of a trailing edge on the high temperature side of the experimental desorption profile (see Figure 3 versus Figure 5). We consistently observe this feature with multiple samples and we believe it arises from the internal diffusion of H_2 within a porous material and more importantly readsorption of H_2 from the gas phase once it is released. Neither effect is considered in the standard Polanyi−Wigner equation. This tail increases the extent of D_2:H_2 overlap and reduces the D_2 enhancement factor. However, we note that in a just accepted manuscript, the temperature profiles for H_2 desorbing from Ni-based MOF-74 do not show such a trailing edge feature.[34] In this case, the system is being dynamically evacuated while heating, which removes the possibility of readsorption and apparently the presence of a trailing edge feature. To test this hypothesis, we performed a series of experiments under identical loading conditions but with a successively larger desorption volume. This reduces the H_2 pressure and thus the rate of readsorption. The desorption profiles presented in Figure S10 show a successively diminished trailing edge feature, confirming that it arises primarily from H_2 readsorption.

SUMMARY

In this article, we present a novel form of temperature-desorption spectroscopy reliant on a pressure gauge in place of a specialized mass-spectrometer. Results for nanoporous material Co_2(dobdc) illustrate the ability of our approach to reveal distinct binding sites within a given material. Simulations based on the Polanyi−Wigner equation indicate that strongly binding energy sites shift the desorption profile toward room temperature, produce a greater difference in the characteristic desorption temperature between D_2 and H_2, but also result in an inherently broader desorption profile. The D_2 enrichment factor is shown to increase dramatically with the fractional difference in binding energy between D_2 and H_2. This suggests that even modest binding energy materials could be highly effective in isotope separation if they possess sites with sharply confining potentials. Experimental results mimic simulation in terms of characteristic temperature difference and desorption profile width. Their D_2 enhancement factor does not reach that of the simulations, and we speculate that this arises from the readsorption inherent to our experimental approach. This could be overcome by continuously removing the desorbed gas during the heating process.

DOI: 10.1021/acs.jpcc.7b11048
J. Phys. Chem. C XXXX, XXX, XXX−XXX

■ ASSOCIATED CONTENT

Supporting Information

The Supporting Information is available free of charge on the ACS Publications website at DOI: 10.1021/acs.jpcc.7b11048.

Instrument schematic, infrared spectra showing H_2 vibrational modes as a function of concentration and temperature, additional temperature-programmed desorption spectra, isosteric heat of adsorption for VSB-5, and desorption profiles for different desorption volumes (PDF)

■ AUTHOR INFORMATION

Corresponding Author

*E-mail: sfgerald@oberlin.edu.

ORCID

Stephen A. Fitzgerald: 0000-0001-9492-9256
Keith V. Lawler: 0000-0003-1087-5815
Paul M. Forster: 0000-0003-3319-4238

Notes

The authors declare no competing financial interest.

■ ACKNOWLEDGMENTS

This research was in part supported by the NSF under Grant CHE-1565961 and sponsored by the Department of Energy, National Nuclear Security Administration under the Stewardship Science Academic Alliances program through DOE Cooperative Agreement DE-NA0001982. We thank Isaac Hietanen, Daniel Mukasa, Enrico Milletti, and Joshua Parker for their help with data acquisition and Bill Mohler and Melinda Keller for their help troubleshooting the apparatus.

■ REFERENCES

(1) Urey, H. C.; Brickwedde, F. G.; Murphy, G. M. A Hydrogen Isotope of Mass 2. *Phys. Rev.* **1932**, *39*, 164−165.

(2) Schoenheimer, R.; Rittenberg, D. Deuterium as an Indicator in the Study of Intermediary Metabolism. *J. Biol. Chem.* **1935**, *111*, 163−168.

(3) Tung, R. D. Deuterium Medicinal Chemistry Comes of Age. *Future Med. Chem.* **2016**, *8*, 491−494.

(4) Harbeson, S. L.; Tung, R. D. Deuterium Medicinal Chemistry: A New Approach to Drug Discovery and Development. *MedChem. News* **2014**, *2*, 8−22.

(5) Miller, A. I. Heavy Water: A Manufacturers' Guide for the Hydrogen Century. *Canadian Nuclear Society Bulletin* **2001**, *22*, 1−14.

(6) Ong, S.; Blagoev, B.; Kratchmarova, I.; Kristensen, D. B.; Steen, H.; Pandey, A.; Mann, M. Stable Isotope Labeling by Amino Acids in Cell Culture, SILAC, as a Simple and Accurate Approach to Expression Proteomics. *Mol. Cell. Proteomics* **2002**, *1*, 376−386.

(7) Thomas, A. F. *Deuterium labeling in organic chemistry*; Appleton-Century-Crofts: United States, 1971.

(8) Trasca, R. A.; Kostov, M. K.; Cole, K. W. Isotopic and Spin Selectivity of H_2 in Bundles of Carbon Nanotubes. *Phys. Rev. B: Condens. Matter Mater. Phys.* **2003**, *67*, 35410−1−35410−8.

(9) Oh, H.; Savchenko, I.; Mavrandonakis, A.; Heine, T.; Hirscher, M. Highly Effective Hydrogen Isotope Separation in Nanoporous Metal-Organic Frameworks with Open Metal Sites: Direct Measurement and Theoretical Analysis. *ACS Nano* **2014**, *8*, 761−770.

(10) FitzGerald, S. A.; Pierce, C. J.; Rowsell, J. L. C.; Bloch, E. D.; Mason, J. A. Highly Selective Quantum Sieving of D_2 from H_2 by a Metal-Organic Framework As Determined by Gas Manometry and Infrared Spectroscopy. *J. Am. Chem. Soc.* **2013**, *135*, 9458−9464.

(11) Oh, H.; Hirscher, M. Quantum Sieving for Separation of Hydrogen Isotopes Using MOFs. *Eur. J. Inorg. Chem.* **2016**, *2016*, 4278−4289.

(12) Li, J. R.; Kuppler, R. J.; Zhou, H. C. Selective Gas Adsorption and Separation in Metal-Organic Frameworks. *Chem. Soc. Rev.* **2009**, *38*, 1477−1504.

(13) Rowsell, J. L. C.; Yaghi, O. M. Metal-Organic Frameworks: A New Class of Porous Materials. *Microporous Mesoporous Mater.* **2004**, *73*, 3−14.

(14) de Jong, A. M.; Niemantsverdriet, J. W. Thermal Desorption Analysis: Comparative Test of Ten Commonly Applied Procedures. *Surf. Sci.* **1990**, *233*, 355−365.

(15) King, D. Thermal Desorption from Metal Surfaces: A Review. *Surf. Sci.* **1975**, *47*, 384−402.

(16) Zhao, Z.; Wang, S.; Yang, Y.; Li, X.; Li, J.; Li, Z. Competitive Adsorption and Selectivity of Benzene and Water Vapor on the Microporous Metal Organic Frameworks (HKUST-1). *Chem. Eng. J.* **2015**, *259*, 79−89.

(17) Chen, Z.; Zhou, D.; Gao, T.; Shen, W.; Dong, X.; Naito, S.; Qin, L.; Huang, Y. Unusual Adsorption and Desorption Behaviors of NO and Co on Nanoporous Nickel Phosphate VSB-5: In situ FT-IR and TPD Study. Catal. *Catal. Today* **2015**, *258*, 199−204.

(18) Panella, B.; Hirscher, M.; Ludescher, B. Low-Temperature Thermal-Desorption Mass Spectroscopy Applied to Investigate the Hydrogen Adsorption on Porous Materials. *Microporous Mesoporous Mater.* **2007**, *103*, 230−234.

(19) Panella, B.; Hönes, K.; Müller, U.; Trukhan, N.; Schubert, M.; Pütter, H.; Hirscher, M. Desorption Studies of Hydrogen in Metal-Organic Frameworks. *Angew. Chem., Int. Ed.* **2008**, *47*, 2138−2142.

(20) Kapelewski, M. T.; Geier, S. J.; Hudson, M. R.; Stück, D.; Mason, J. A.; Nelson, J. N.; Xiao, D. J.; Hulvey, Z.; Gilmour, E.; FitzGerald, S. A.; et al. M_2(*m*-dobdc) (M = Mg, Mn, Fe, Co, Ni) Metal-Organic Frameworks Exhibiting Increased Charge Density and Enhanced H_2 Binding at the Open Metal Sites. *J. Am. Chem. Soc.* **2014**, *136*, 12119−12129.

(21) Pang, S. H.; Han, C.; Sholl, D. S.; Jones, C. W.; Lively, R. P. Facet-Specific Stability of ZIF-8 in the Presence of Acid Gases Dissolved in Aqueous Solutions. *Chem. Mater.* **2016**, *28*, 6960−6967.

(22) Forster, P. M.; Eckert, J.; Chang, J.-S.; Park, S.-E.; Férey, G.; Cheetham, A. K. Hydrogen Adsorption in Nanoporous Nickel(II) Phosphates. *J. Am. Chem. Soc.* **2003**, *125*, 1309−1312.

(23) FitzGerald, S. A.; Churchill, H. O. H.; Korngut, P. M.; Simmons, C. B.; Strangas, Y. E. Cryogenic Apparatus for Diffuse Reflection Infrared Spectroscopy with High-Pressure Capabilities. *Rev. Sci. Instrum.* **2006**, *77*, 093110−1−093110−4.

(24) Liu, Y.; Kabbour, H.; Brown, C. M.; Neumann, D. A.; Ahn, C. C. Increasing the Density of Adsorbed Hydrogen with Coordinatively Unsaturated Metal Centers in Metal-Organic Frameworks. *Langmuir* **2008**, *24*, 4772−4777.

(25) Rosi, N.; Kim, J.; Eddaoudi, M.; Chen, B.; O'Keeffe, M.; Yaghi, O. M. Rod Packings and MetalOrganic Frameworks Constructed from Rod-Shaped Secondary Building Units. *J. Am. Chem. Soc.* **2005**, *127*, 1504−1518.

(26) Dietzel, P.; Johnsen, R. E.; Blom, R.; Fjellvag, H. Structural Changes and Coordinatively Unsaturated Metal Atoms on Dehydration of Honeycomb Analogous Microporous MetalOrganic Frameworks. *Chem. - Eur. J.* **2008**, *14*, 2389−2397.

(27) FitzGerald, S. A.; Burkholder, B.; Friedman, M.; Hopkins, J. B.; Pierce, C. J.; Schloss, J. M.; Thompson, B.; Rowsell, J. L. C. Metal-Specific Interactions of H_2 Adsorbed within Isostructural Metal-Organic Frameworks. *J. Am. Chem. Soc.* **2011**, *133*, 20310−20318.

(28) Weinrauch, I.; Savchenko, I.; Denysenko, D.; Souliou, S. M.; Kim, H.; Le Tacon, M.; Daemen, L. L.; Cheng, Y.; Mavrandonakis, A.; Ramirez-Cuesta, A. J.; et al. Capture of Heavy Hydrogen Isotopes in a Metal-Organic Framework with active Cu(I) sites. *Nat. Commun.* **2017**, *8*, 14496.

(29) Wang, P. Y.; Challa, S. R.; Sholl, D. S.; Johnson, J. K. Quantum Sieving in Carbon Nanotubes and Zeolites. *Phys. Rev. Lett.* **1999**, *82*, 956−959.

(30) Zhou, W.; Wu, H.; Hartman, M. R.; Yildirim, T. Hydrogen and Methane Adsorption in Metal-Organic Frameworks: A High-Pressure Volumetric Study. *J. Phys. Chem. C* **2007**, *111*, 16131−16137.

DOI: 10.1021/acs.jpcc.7b11048
J. Phys. Chem. C XXXX, XXX, XXX−XXX

(31) Sharma, A.; Lawler, K. V.; Wolffis, J. J.; Eckdahl, C. T.; McDonald, C. S.; Rowsell, J. L.; FitzGerald, S. A.; Forster, P. M. Hydrogen Uptake on Coordinatively Unsaturated Metal Sites in VSB-5 Revisited: Strong Binding Affinity Leading to High Temperature D_2/H_2 Selectivity. *Langmuir* **2017**, *33*, 14586−14591.
(32) Park, K. S.; Ni, Z.; Cote, A. P.; Choi, J. Y.; Huang, R.; Uribe-Romo, F. J.; Chae, H. K.; O'Keeffe, M.; Yaghi, O. M. Exceptional Chemical and Thermal Stability of Zeolitic Imidazolate Frameworks. *Proc. Natl. Acad. Sci. U. S. A.* **2006**, *103*, 10186−10191.
(33) Guillou, N.; Gao, Q.; Forster, P. M.; Chang, J.-S.; Noguès, M.; Park, S.-E.; Férey, G.; Cheetham, A. K. Nickel(II) Phosphate VSB-5: A Magnetic Nanoporous Hydrogenation Catalyst with 24-Ring Tunnels. *Angew. Chem., Int. Ed.* **2001**, *40*, 2831−2834.
(34) Kim, J. Y.; Balderas-Xicohtencatl, R.; Zhang, L.; Kang, S. G.; Hirscher, M.; Oh, H.; Moon, H. R. Exploiting Diffusion Barrier and Chemical Affinity of Metal-Organic Frameworks for Efficient Hydrogen Isotope Separation. *J. Am. Chem. Soc.* **2017**, *139*, 15135−15141.

DOI: 10.1021/acs.jpcc.7b11048
J. Phys. Chem. C XXXX, XXX, XXX−XXX